

UCSF

UC San Francisco Previously Published Works

Title

Timing of diffusion tensor imaging in the management of a ruptured pediatric arteriovenous malformation: illustrative case.

Permalink

<https://escholarship.org/uc/item/7c22r4gx>

Authors

Chen, Jia-Shu
Caldwell, David
Falcone, Joseph
et al.

Publication Date

2024-08-19

DOI

10.3171/CASE24225

Peer reviewed

Timing of diffusion tensor imaging in the management of a ruptured pediatric arteriovenous malformation: illustrative case

Jia-Shu Chen, MD,^{1,2} David J. Caldwell, MD, PhD,² Joseph A. Falcone, MD,^{2,3} Cecilia Dalle Ore, MD,² Vanitha Sankaranarayanan, MS,⁴ Felix Liu, MS,⁴ Steven W. Hetts, MD,^{2,4} Winson S. Ho, MD,^{2,3} and Nalin Gupta, MD, PhD^{2,3}

¹The Warren Alpert Medical School of Brown University, Providence, Rhode Island; and Departments of ²Neurological Surgery, ³Pediatrics, and ⁴Radiology and Biomedical Imaging, University of California, San Francisco, California

BACKGROUND Diffusion tensor imaging (DTI) can characterize eloquent white matter tracts affected by brain arteriovenous malformations (AVMs). However, DTI interpretation can be difficult in ruptured cases due to the presence of blood products. The authors present the case of a ruptured pediatric AVM in the corticospinal tract (CST) and discuss how DTI at different time points informed the treatment.

OBSERVATIONS A 9-year-old female presented with a sudden headache and left hemiparesis. She was found to have a Spetzler-Martin grade III, Supplementary grade I AVM in the right caudate and centrum semiovale, with obliteration and corresponding reduced fractional anisotropy (FA), fiber density (FD), and tract count (TC) of the adjacent CST on DTI. The patient remained stable and was scheduled for elective resection following a 6-week period to facilitate hematoma resorption. After 6 weeks, repeat DTI showed part of the nidus within intact CST fibers with concordant improvement in FA, FD, and TC. Considering the nidus location, CST integrity, and motor function recovery, surgery was deferred in favor of stereotactic radiosurgery.

LESSONS In ruptured AVMs, DTI may initially create an incomplete picture and false assumptions about white matter tract integrity. DTI should be repeated if delayed treatment is appropriate to ensure informed decision-making and prevent avoidable permanent neurological deficits.

<https://thejns.org/doi/abs/10.3171/CASE24225>

KEYWORDS arteriovenous malformation; corticospinal tract; diffusion tensor imaging; pediatric; resection; stereotactic radiosurgery; tractography

Arteriovenous malformations (AVMs) are the leading cause of spontaneous intracerebral hemorrhage in children.¹ Additionally, pediatric AVMs are frequently located in eloquent, deep-seated regions with exclusive deep venous drainage.² As a result, ruptured AVMs in children can cause substantial morbidity and mortality. Furthermore, children with untreated ruptured AVMs have an increased risk of rehemorrhage.³ Accurate diagnostic evaluation and well-informed selection of a treatment modality that appropriately balances the likelihood of AVM obliteration and the risk of postoperative complications is thus essential.

While microsurgical resection and stereotactic radiosurgery (SRS) can both cure AVMs, microsurgery offers the possibility of immediate cure, whereas SRS is less effective for larger lesions and has a latency period of 1–3 years.^{4,5} Although AVM rehemorrhage can occur during SRS latency, open surgery is associated with greater operative morbidity and a longer recovery.⁶ For these reasons, SRS is often recommended for deep-seated lesions or those adjacent to eloquent

structures. Low- and medium-grade AVMs with questionable involvement of eloquent cortex and white matter tracts present unique challenges in deciding the appropriate treatment modality.⁷

While diagnostic assessment usually includes magnetic resonance imaging (MRI) and digital subtraction angiography (DSA), neither can identify functional white matter tracts and their spatial orientation relative to the AVM.⁷ Diffusion tensor imaging (DTI) has been used to visualize fiber tracts and aid in surgical decision-making for eloquent AVMs.⁸ However, DTI is difficult to interpret in cases of AVM rupture because the hematoma displaces surrounding brain anatomy and creates magnetic susceptibility artifacts that decrease signal intensity around the AVM nidus.^{7–9} Accurate interpretation of DTI in the setting of AVM rupture that properly accounts for shifted anatomy and altered signal is thus essential to making informed therapeutic decisions and avoiding treatment-related morbidity.

We describe the case of a child with a ruptured AVM in the corticospinal tract (CST). On initial DTI, it appeared that the hemorrhage

ABBREVIATIONS AVM = arteriovenous malformation; CST = corticospinal tract; CT = computed tomography; CTA = CT angiography; DSA = digital subtraction angiography; DTI = diffusion tensor imaging; FA = fractional anisotropy; FD = fiber density; MRA = magnetic resonance angiography; MRI = magnetic resonance imaging; ROI = region of interest; SM = Spetzler-Martin; SRS = stereotactic radiosurgery; Supp = supplementary; TC = tract count; TR/TE = repetition time/echo time.

INCLUDE WHEN CITING Published August 19, 2024; DOI: 10.3171/CASE24225.

SUBMITTED March 29, 2024. **ACCEPTED** June 10, 2024.

© 2024 The authors, CC BY-NC-ND 4.0 (<http://creativecommons.org/licenses/by-nc-nd/4.0/>)

had obliterated part of the CST and that the AVM could be approached surgically without jeopardizing the residual intact fibers. However, after a recovery period and repeat DTI, it was recognized that the AVM nidus could not be surgically removed without the risk of damaging the remaining CST fibers, resulting in postoperative motor deficits. This case demonstrates that while DTI can be an invaluable adjunct to surgical planning for AVMs, a hematoma in the setting of acute rupture can influence the appearance of DTI and lead to false assumptions about important white matter tracts.

Illustrative Case

Initial Presentation

A 9-year-old, right-handed female presented to an emergency department after waking up with a severe headache associated with new left hemibody weakness. On initial examination, the patient was alert and oriented with fluent speech and intact visual fields and acuity. However, she was hemiparetic on the left with worse upper-extremity weakness and a lower facial droop. A noncontrast computed tomography (CT) scan demonstrated a $2.8 \times 4.6 \times 3.6$ -cm intraparenchymal hematoma in the right putamen and external capsule (Fig. 1A). The hematoma extended into the corona radiata and centrum semiovale and exerted 3 mm of leftward midline shift. Subsequent CT angiography (CTA) showed a small hyperdensity suspicious for a vascular malformation supplied by the lateral lenticulostriate arteries and drained by the caudate vein (Fig. 1B and C).

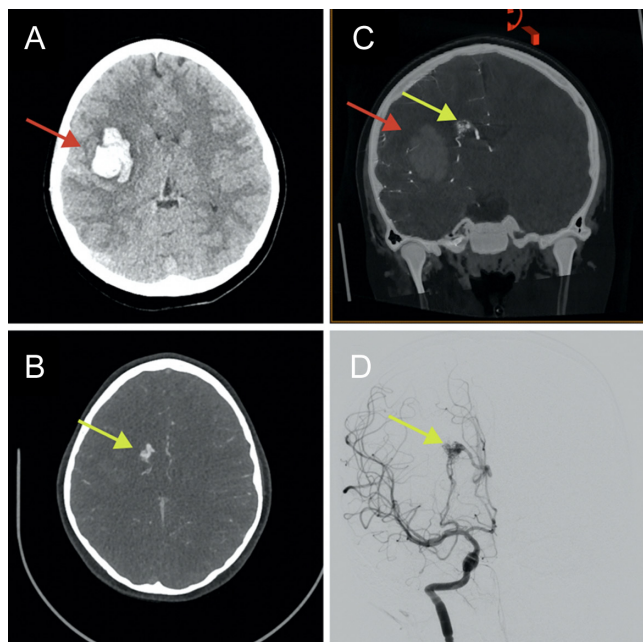


FIG. 1. Imaging of the AVM at the time of initial presentation. **A:** Axial noncontrast head CT scan on admission demonstrating acute, right-sided intraparenchymal hemorrhage at the putamen (red arrow). **B:** Axial CTA showing a hyperdensity (yellow arrow) concerning for a vascular malformation. **C:** Coronal noncontrast CT scan merged with the angiogram demonstrating the hematoma (red arrow) as well as the AVM with lenticulostriate feeders and drainage via the caudate vein (yellow arrow). **D:** Right internal carotid artery (ICA) injection and anteroposterior view during initial angiography demonstrating a right AVM with deep drainage (yellow arrow).

Following transfer to our institution, DSA on the same day of presentation demonstrated a $1.5 \times 0.9 \times 0.9$ -cm AVM nidus within the right caudate nucleus and centrum semiovale. It was supplied by 2 lateral lenticulostriate arteries arising from the proximal anterior M2 and distal M1 segments (Fig. 1D). Venous outflow led from the caudate vein into the internal cerebral vein and deep venous system. The lesion was graded as a Spetzler-Martin (SM) grade III (< 3 cm, eloquent, deep venous drainage), Supplementary (Supp) grade I (age < 20 years) AVM for a total SM-Supp score of IV.¹⁰

MRI, including magnetic resonance angiography (MRA) and DTI, was performed using a 3.0-T MR scanner (Ingenia, Philips Healthcare). DTI was acquired using a single-shot spin-echo echo-planar imaging technique with the following parameters: repetition time/echo time (TR/TE) of 3730/89 msec, 15 diffusion directions, and a b-value of 1000 sec/mm^2 . DTI and MRA were fused with MRI sequences through iPlan 3.0 (Brainlab AG). DTI datasets were corrected for movement and eddy-current distortions using FSL (University of Oxford).¹¹ The original gradient table was consequently rotated.¹² Regions of interest (ROIs) were segmented in the cerebral peduncles for tractography seeding. Dipy software was used to estimate fractional anisotropy (FA) and for residual bootstrap q-ball fiber tracking.¹³ The final motor tracts were manually pruned using TrackVis and then converted to pixel-wise segmentations on anatomical MR images so that they could be registered to DSA images using the FSL linear registration tool.¹⁴ The DTI, DSA, and MR or CT images were fused together using in-house Python software to juxtapose the anatomy of the AVM nidus, hematoma, and vasculature with the surrounding white matter tracts. Imaging confirmed the location and vascular supply of the AVM nidus and hematoma (Fig. 2A–C). Surrounding white matter tract integrity on DTI, as defined by FA, fiber density (FD), and tract count (TC), was reduced on the affected right CST relative to the left (Table 1 and Fig. 2C). The fused CT, DSA, and DTI tracts corresponded to the quantification by depicting unconsolidated fibers directly adjacent to the AVM nidus that were suggestive of local obliteration (Video 1 and Fig. 3A). The patient improved and regained left motor function to a near-baseline level (4+/5). The patient was discharged and scheduled for elective microsurgical resection 6 weeks later.^{15,16}

VIDEO 1. Clip showing the complete axial study of the patient's fused brain CT, DSA, and DTI tractography at initial presentation. A=anterior; P=posterior; R=right. [Click here to view.](#)

Follow-Up Presentation

Prior to surgery, DSA and MRI/MRA with DTI (Signa, General Electric Medical Systems) were repeated to redefine the nidus and surrounding anatomy for surgical planning. Repeat DTI used the aforementioned technique but with different parameters (TR/TE of 9000/101 msec, 55 diffusion directions, b-value of 2000 sec/mm^2). This scan used a preoperative MR navigation protocol, whereas the initial scan used a diagnostic protocol. The integrity measures (e.g., FA, FD, and TC) of the affected right CST showed improvement over time (Table 1 and Fig. 2F), although they remained inferior to those of the unaffected left CST, which showed no change during the rest period (Table 1). Concordantly, the right CST was better visualized on the delayed imaging, and it was clear that the nidus was partially located and intertwined within the deep white matter, primarily medial to the CST (Fig. 4). Fusion of DTI, MRI, and DSA confirmed that the CST fibers were not obliterated and were significantly more consolidated than previously observed (Video 2 and Fig. 3B). As part of the preoperative planning, we evaluated several possible approaches to

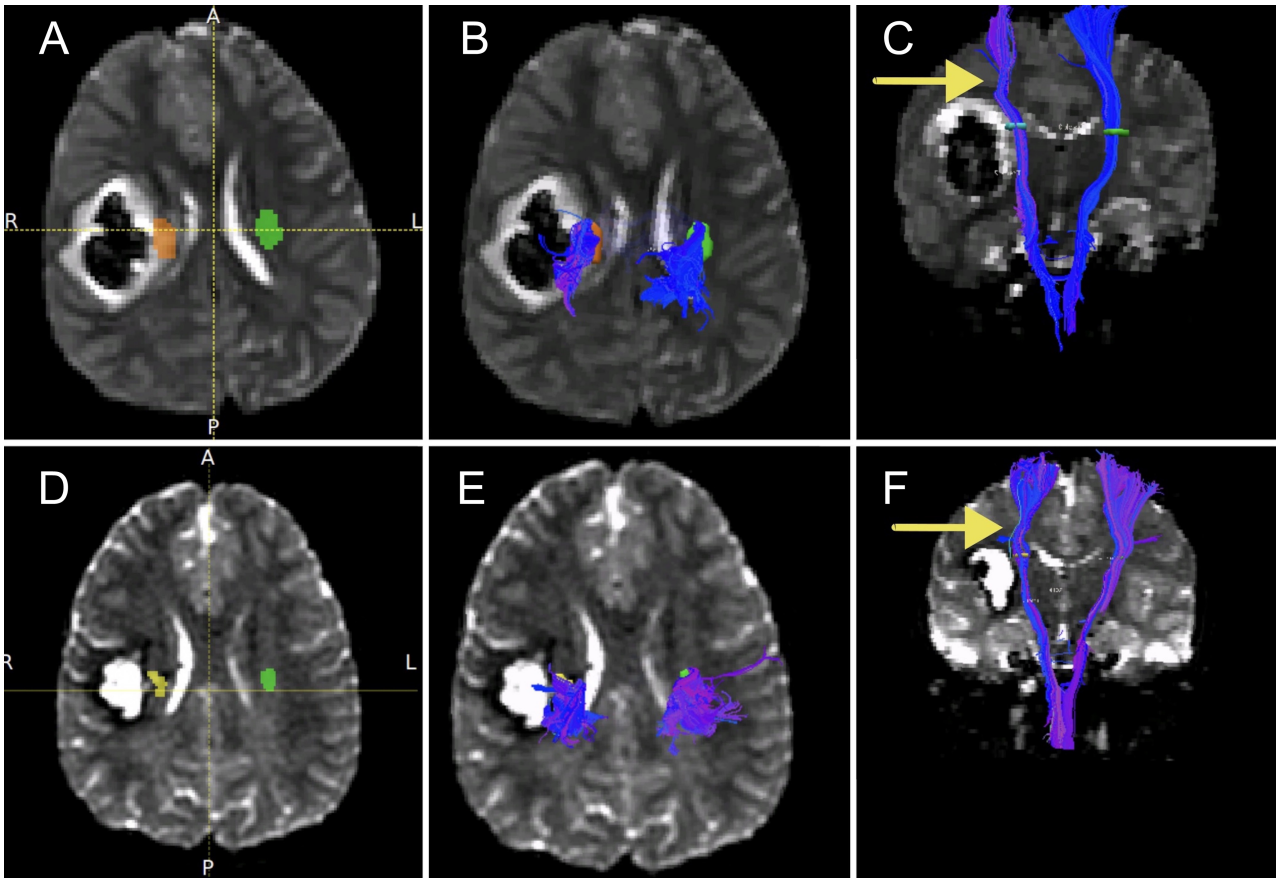


FIG. 2. Immediate and delayed CST and motor cortex appearance on DTI. ROIs defined for right (orange) and left (green) CST seeding at the time of initial presentation on axial T2-weighted MRI (A), as well as the projected fibers in axial (B) and coronal (C) views. The decreased density of white matter tracts on the injured right compared to the contralateral side is highlighted by the yellow arrow (C). ROIs of the right (yellow) and left (green) CST 2 months after initial presentation (D) and projected fibers in axial (E) and coronal (F) views. The difference in fiber tract density is less apparent, but still appreciable, at this time and is highlighted again by the yellow arrow (F).

the nidus, but all would have required either traversing intact CST fibers that were previously thought to be safe to perform an excision around¹⁷ or approaching the nidus through a long transcortical route. It was determined that surgery had an increased risk of additional motor deficits, and treatment with SRS was recommended. The patient underwent SRS at a dose of 19 Gy to the 50% isodose line, with a target volume of 0.49 cm³ and a prescription isodose volume of 0.61 cm³. At the 10-month follow-up after initial presentation, the patient was clinically stable with effectively full left-sided strength.

VIDEO 2. Clip showing the complete axial study of the patient's fused brain MRI, DSA, and DTI tractography at follow-up presentation. L = left. [Click here to view.](#)

Patient Informed Consent

The necessary patient informed consent was obtained in this study.

Discussion

Observations

The management of ruptured AVMs in children remains a topic of debate among neurosurgeons and can vary based on individual surgeon preferences and experience.¹⁸ However, a shared principle in

treatment decision-making for AVMs is to avoid new deficits, particularly involving motor or language function.¹⁹ While there is substantial literature describing the evaluation of AVMs that involve the motor cortex, there has been less investigation into AVMs within the white matter of motor pathways.¹⁹⁻²³ DTI helps demonstrate the anatomical relationship between the AVM nidus and motor tracts.^{7,22,24} However, the integrity of these tracts can be difficult to assess immediately following an intraparenchymal hemorrhage. In this case, we observed improvements in the ability to quantify and visualize CST integrity

TABLE 1. Immediate and delayed DTI quantification of ipsilateral and contralateral CST integrity following acute hemorrhagic rupture of an AVM

	Rt Affected Hemisphere		Lt Unaffected Hemisphere	
	Immediate	Delayed	Immediate	Delayed
Mean FA	0.32 ± 0.09	0.37 ± 0.12	0.54 ± 0.10	0.51 ± 0.04
FD	161.68	199.73	234.35	235.4
TC	6,467	8,988	9,374	10,593

Values are expressed as the mean ± standard deviation, unless indicated otherwise. All values represent the number of tracts per voxel.

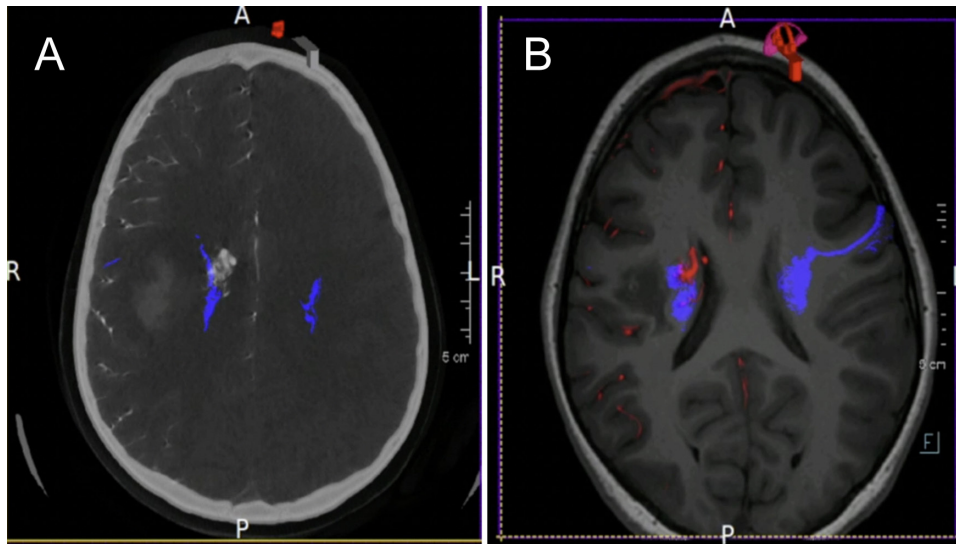


FIG. 3. Axial slices of the patient's fused structural brain imaging, angiographic studies, and tractography at initial and delayed presentation. Comparison of the initial CT, DSA, and DTI tractography fusion (**A**) and follow-up MRI, DSA, and DTI tractography fusion (**B**) demonstrate that the CST integrity is more robust and the fibers are encasing the AVM nidus on the delayed repeat imaging.

on the affected right side 6 weeks following the initial presentation, although the FA, FD, and TC were not completely restored relative to those of the contralateral side. The most likely technical explanation for this is that the single-shot acquisition technique is associated with magnetic susceptibility artifacts in the setting of acute hemorrhage that

cause iron-mediated signal intensity drop-off.^{8,25} Some investigators also report that a greater number of diffusion directions result in better quality tractography. It could be argued that the lower number of directions used during our initial acquisition resulted in reduced image quality. However, this is less likely to be an issue because the other parameters (e.g., b-value) were scaled and optimized so that the DTI data were comparable and equivalent across scans.²⁵ In addition, the FA, FD, and TC of the unaffected left hemisphere were stable across scans, suggesting that the hematoma, not the parameters, was the source of the discrepancy. Finally, several studies suggest that after a certain number of directions (12–16), increasing the number of diffusion directions does not result in any meaningful improvement in DTI quality.^{8,25} Overall, little is currently known about how the time from hemorrhagic rupture affects tractography visualization and diffusion anisotropy, but this case provides evidence that the quality and reliability of DTI findings when using our particular imaging technique improve over time.²⁶

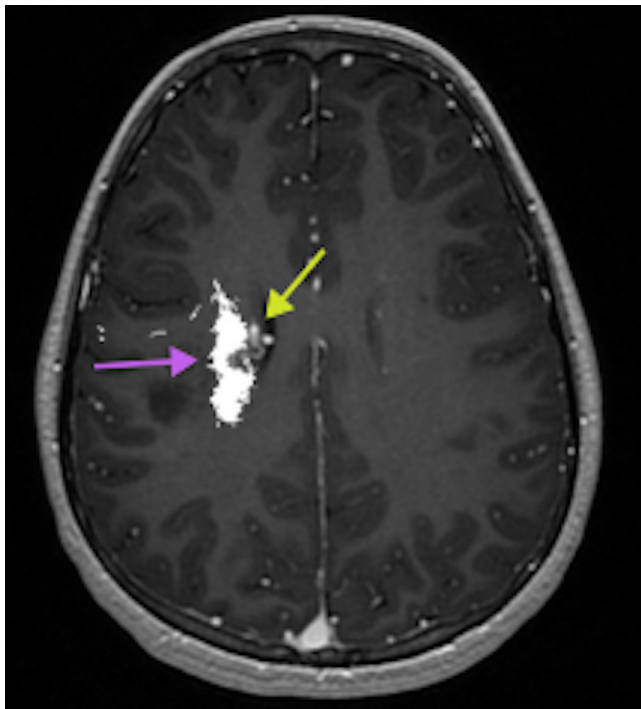


FIG. 4. Delayed axial CST and AVM nidus appearance and spatial relationship on DTI. The AVM nidus (yellow arrow) is distinctly embedded within the right CST fibers (purple arrow).

While still a topic of debate, one current treatment paradigm for patients with a ruptured AVM but stable or improving functional deficits is to undergo an observation period before definitive treatment so that functional recovery can be optimized.^{7,15,27} The thought is that the friability of the parenchyma immediately after rupture can increase the risk of damaging the surrounding structures intraoperatively and causing permanent neurological deficits.¹⁵ Conversely, those in support of early surgery argue that rupture facilitates better resection by providing a wider surgical corridor from the hematoma cavity and spares the patient an extra recovery period from delayed surgery.²⁷ While a large retrospective study demonstrated that surgical outcomes are not affected by the elapsed time from rupture to surgery, this case argues that an observation period may provide improved DTI data, which could modify initial treatment decisions.²⁷ Delaying surgery and repeating imaging to acquire more accurate information may be especially important in cases in which the hematoma is not life-threatening and the nidus is presumed to affect white matter tracts, given the association of intervention on white matter tracts

with higher rates of postoperative motor deficits and longer recovery times.²⁸ Further investigation into the temporal relationship between DTI quality and hemorrhage, as well as whether alternative imaging techniques can mitigate these limitations, is needed to help guide the clinical utility and interpretability of DTI in AVMs that involve eloquent white matter tracts.

Lessons

This case demonstrates that early imaging and tractography of ruptured AVMs affecting white matter tracts are susceptible to inaccuracies in characterizing the nature of the AVM nidus and eloquent pathways. DTI at the time of presentation should be interpreted with caution to avoid false assumptions about the integrity of potentially injured white matter tracts. If the patient is a good candidate for delayed surgical treatment, it would be advantageous to perform repeat DTI prior to surgery to allow for better-informed treatment decision-making. This is because new and more reliable information on the AVM may be elucidated and influence which of the various AVM treatment modalities are best suited for the patient's clinical picture.

References

1. Meyer-Heim AD, Boltshauser E. Spontaneous intracranial haemorrhage in children: aetiology, presentation and outcome. *Brain Dev.* 2003;25(6):416-421.
2. Hetts SW, Cooke DL, Nelson J, et al. Influence of patient age on angioarchitecture of brain arteriovenous malformations. *AJNR Am J Neuroradiol.* 2014;35(7):1376-1380.
3. Derdeyn CP, Zipfel GJ, Albuquerque FC, et al. Management of brain arteriovenous malformations: a scientific statement for healthcare professionals from the American Heart Association/American Stroke Association. *Stroke.* 2017;48(8):e200-e224.
4. Starke RM, Ding D, Kano H, et al. International multicenter cohort study of pediatric brain arteriovenous malformations. Part 2: Outcomes after stereotactic radiosurgery. *J Neurosurg Pediatr.* 2017;19(2):136-148.
5. Winkler EA, Lu A, Morshed RA, et al. Bringing high-grade arteriovenous malformations under control: clinical outcomes following multimodality treatment in children. *J Neurosurg Pediatr.* 2020;26(1):82-91.
6. Gross BA, Storey A, Orbach DB, Scott RM, Smith ER. Microsurgical treatment of arteriovenous malformations in pediatric patients: the Boston Children's Hospital experience. *J Neurosurg Pediatr.* 2015;15(1):71-77.
7. Ellis MJ, Rutka JT, Kulkarni AV, Dirks PB, Widjaja E. Corticospinal tract mapping in children with ruptured arteriovenous malformations using functionally guided diffusion-tensor imaging. *J Neurosurg Pediatr.* 2012;9(5):505-510.
8. Kikuta K, Takagi Y, Nozaki K, et al. Early experience with 3-T magnetic resonance tractography in the surgery of cerebral arteriovenous malformations in and around the visual pathway. *Neurosurgery.* 2006;58(2):331-337.
9. Okada T, Miki Y, Kikuta K, et al. Diffusion tensor fiber tractography for arteriovenous malformations: quantitative analyses to evaluate the corticospinal tract and optic radiation. *AJNR Am J Neuroradiol.* 2007;28(6):1107-1113.
10. Kim H, Abila AA, Nelson J, et al. Validation of the supplemented Spetzler-Martin grading system for brain arteriovenous malformations in a multicenter cohort of 1009 surgical patients. *Neurosurgery.* 2015;76(1):25-33.
11. Jenkinson M, Beckmann CF, Behrens TE, Woolrich MW, Smith SM. FSL. *Neuroimage.* 2012;62(2):782-790.
12. Leemans A, Jones DK. The B-matrix must be rotated when correcting for subject motion in DTI data. *Magn Reson Med.* 2009;61(6):1336-1349.
13. Berman JI, Chung S, Mukherjee P, Hess CP, Han ET, Henry RG. Probabilistic streamline q-ball tractography using the residual bootstrap. *Neuroimage.* 2008;39(1):215-222.
14. Jenkinson M, Smith S. A global optimisation method for robust affine registration of brain images. *Med Image Anal.* 2001;5(2):143-156.
15. Zacharia BE, Vaughan KA, Jacoby A, Hickman ZL, Bodmer D, Connolly ES Jr. Management of ruptured brain arteriovenous malformations. *Curr Atheroscler Rep.* 2012;14(4):335-342.
16. Ogilvy CS, Stieg PE, Awad I, et al. Recommendations for the management of intracranial arteriovenous malformations: a statement for healthcare professionals from a special writing group of the Stroke Council, American Stroke Association. *Stroke.* 2001;32(6):1458-1471.
17. Jellison BJ, Field AS, Medow J, Lazar M, Salamat MS, Alexander AL. Diffusion tensor imaging of cerebral white matter: a pictorial review of physics, fiber tract anatomy, and tumor imaging patterns. *AJNR Am J Neuroradiol.* 2004;25(3):356-369.
18. McDowell MM, Agarwal N, Mao G, et al. Long-term outcomes of pediatric arteriovenous malformations: the 30-year Pittsburgh experience. *J Neurosurg Pediatr.* 2020;26(3):275-282.
19. Li M, Jiang P, Guo R, et al. A tractography-based grading scale of brain arteriovenous malformations close to the corticospinal tract to predict motor outcome after surgery. *Front Neurol.* 2019;10:761.
20. Alkadhi H, Kollias SS, Crelier GR, Golay X, Hepp-Reymond MC, Valavanis A. Plasticity of the human motor cortex in patients with arteriovenous malformations: a functional MR imaging study. *AJNR Am J Neuroradiol.* 2000;21(8):1423-1433.
21. Lee L, Sitoh YY, Ng I, Ng WH. Cortical reorganization of motor functional areas in cerebral arteriovenous malformations. *J Clin Neurosci.* 2013;20(5):649-653.
22. Yamada K, Kizu O, Ito H, et al. Tractography for arteriovenous malformations near the sensorimotor cortices. *AJNR Am J Neuroradiol.* 2005;26(3):598-602.
23. Byrnes TJ, Barrick TR, Bell BA, Clark CA. Semiautomatic tractography: motor pathway segmentation in patients with intracranial vascular malformations. Clinical article. *J Neurosurg.* 2009;111(1):132-140.
24. Yamada K, Kizu O, Mori S, et al. Brain fiber tracking with clinically feasible diffusion-tensor MR imaging: initial experience. *Radiology.* 2003;227(1):295-301.
25. Nogueroles TM, Barousse R, Amrhein TJ, Royuela-Del-Val J, Montesinos P, Luna A. Optimizing diffusion-tensor imaging acquisition for spinal cord assessment: physical basis and technical adjustments. *Radiographics.* 2020;40(2):403-427.
26. Waqas M, Siddiqui A, Mubarak F, Enam SA. Diffusion tensor imaging for ruptured cerebral arteriovenous malformation. *Cureus.* 2017;9(9):e1721.
27. Hafez A, Oulasvirta E, Koroknay-Pál P, Niemelä M, Hernesniemi J, Laakso A. Timing of surgery for ruptured supratentorial arteriovenous malformations. *Acta Neurochir (Wien).* 2017;159(11):2103-2112.
28. Jiao Y, Li H, Fu W, et al. Classification of brain arteriovenous malformations located in motor-related areas based on location and anterior choroidal artery feeding. *Stroke Vasc Neurol.* 2021;6(3):441-448.

Disclosures

The authors report no conflict of interest concerning the materials or methods used in this study or the findings specified in this paper.

Author Contributions

Conception and design: Gupta, Caldwell, Falcone. Acquisition of data: Chen, Sankaranarayanan, Liu, Hetts. Analysis and interpretation of

data: Gupta, Chen, Caldwell, Falcone, Sankaranarayanan, Liu. Drafting the article: Gupta, Chen, Caldwell, Falcone, Sankaranarayanan. Critically revising the article: Gupta, Chen, Caldwell, Falcone, Dalle Ore, Sankaranarayanan, Liu, Ho. Reviewed submitted version of manuscript: Gupta, Chen, Caldwell, Falcone, Dalle Ore, Sankaranarayanan, Liu, Hetts. Approved the final version of the manuscript on behalf of all authors: Gupta. Statistical analysis: Chen, Liu. Administrative/technical/material support: Liu. Study supervision: Gupta.

Supplemental Information

Videos

Video 1. <https://vimeo.com/957769152>.

Video 2. <https://vimeo.com/957772669>.

Correspondence

Nalin Gupta: University of California, San Francisco, CA. nalin.gupta@ucsf.edu.